Predicting the Fatigue Properties of A356 Cast Aluminium Alloy Wheel Rim in Various Post Treatment Conditions with a Simple Monotonic Tensile Test

H. Jacobs[a], L. Pretorius[b], R.F. Laubscher[b]

Cast aluminium alloys such as A356 may experience various defects such as segregation and non-homogeneous material properties largely as a result of directional solidification during casting.

Determining the fatigue properties of the material at different positions in a finished wheel is expensive and time consuming. This paper describes a comparison of various prediction techniques to relate actual fatigue data to monotonic tensile material tests. It was found that the original universal slopes method proposed by Manson gave the best first approximation of the fatigue life as well as being the most conservative of all the methods proposed. Furthermore, it was noticed that the painting process has a beneficial effect on the fatigue properties.

Chemical element	Si	Mg	Ti	Sr	Fe	Cu	Na	Al
Percentage of element	7.0 -	0.23 -	0.10 -	0.0161 -	0.13 -	0.01 -	0.001 -	Rest
	7.68%	0.27%	0.137%	0.0178%	0.14%	0.02%	0.002%	

Table 1. Typical chemical composition for A356 cast aluminium as used in this project

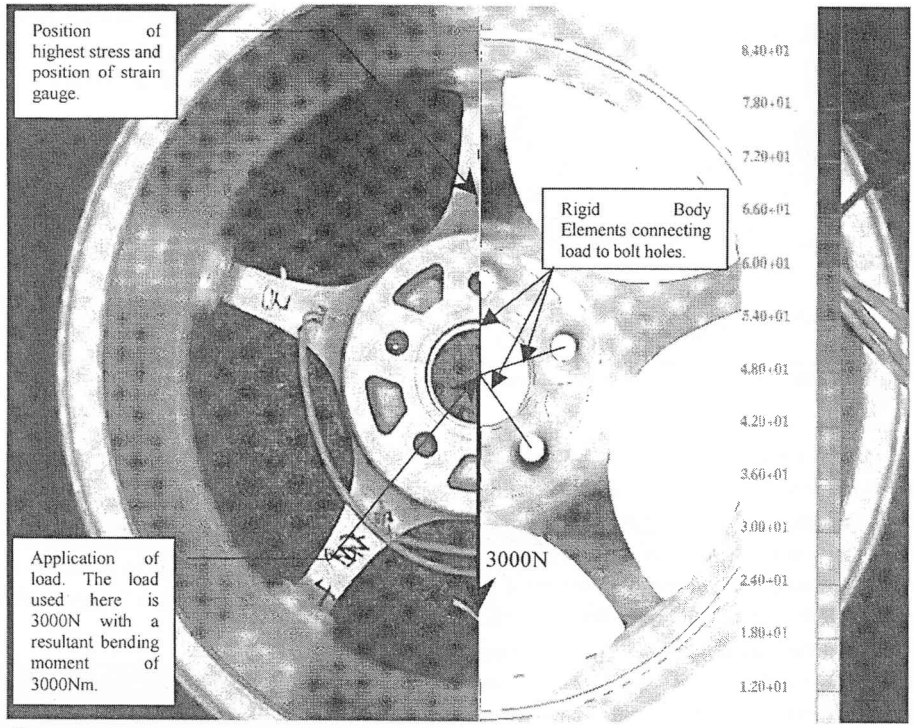

Figure 1. Strain gauged wheel with Von Mises stress plot obtained with FEA

Nomenclature

N_f Cycles to failure using the approximate methods, with 2 . N_f the reversals to failure

N_{true} Cycles to failure using the fatigue performed on the wheel, with 2 . N_{true} the reversals to failure

γ_{XY} Shear strain on xy-surface, [1/1]

$\Delta\varepsilon_T$ Alternating total strain range for a zero mean strain, [1/1]

ε_{eng} Engineering strain during monotonic tensile test, [1/1]

ε_{eq} Equivalent strain, [1/1]

ε_f Fracture ductility or true fracture strain, [1/1]

ε_X Axial strain in x-direction, [1/1]

ε_Y Axial strain in y-direction, [1/1]

σ_{eq} Equivalent stress, [MPa]

σ_f True fracture stress during a monotonic tensile test, [MPa]

σ_{uts} Ultimate tensile strength, [MPa]

σ_X Axial stress in x-direction, [MPa]

σ_{yield} Yield strength, [MPa]

σ_Y Axial stress in y-direction, [MPa]

τ_{XY} Shear stress on xy-surface, [MPa]

τ_{XY} Shear stress on xy-surface, [MPa]

Introduction

The automotive industry uses cast aluminium in numerous components of which wheel rims are the most noticeable safety critical component. Cast aluminium is prone to various defects such as pores created by dissolved gasses, local hot spots in the wheel and bad foundry practices that may also lead to

[a] Tiger Wheels Manufacturing, 13th Street Babelegi, South Africa, Post graduate student at Rand Afrikaans University.
Rand Afrikaans University, South Africa.

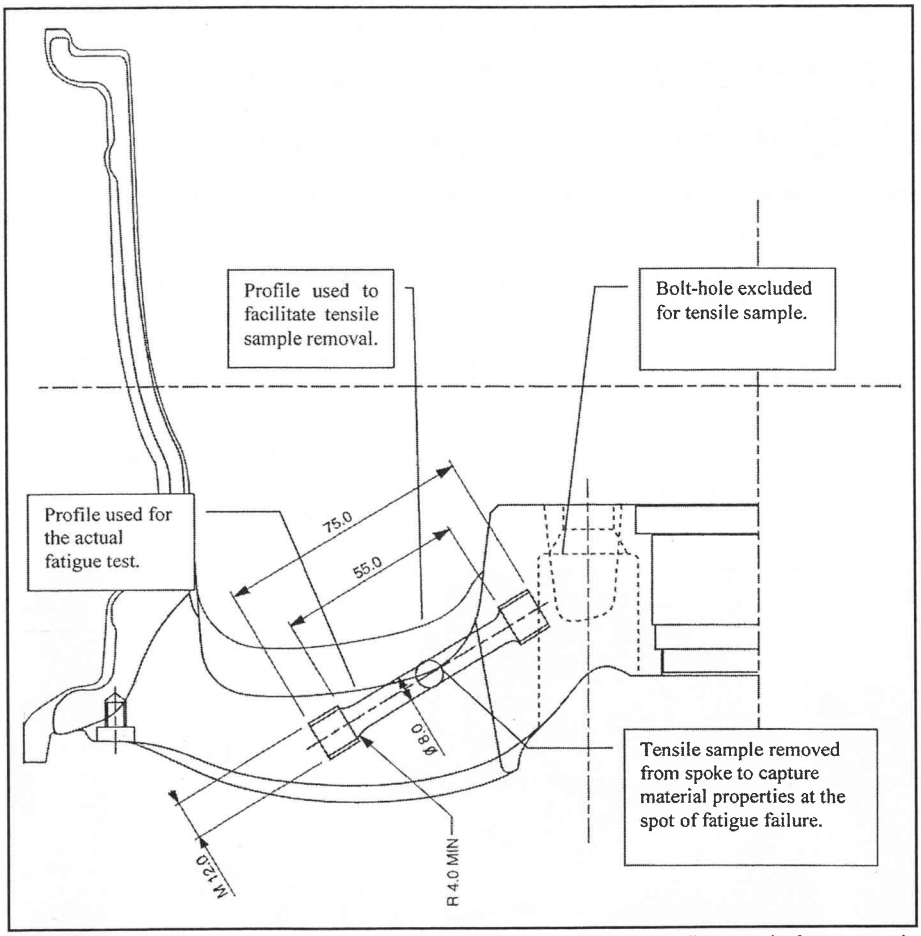

Figure 2. Schematic drawing showing the position of monotonic tensile sample for removal

entrapped oxides. Exposed pores and entrapped oxides have been shown to be the preferred crack initiation site.[1,2] The fatigue testing of a wheel involves the complete wheel being tested to crack initiation or to total destruction. This type of test will in most cases capture the material properties in only one position, in rare instances a second and third position on the wheel will be captured. To establish a stress versus cycle or S-N curve using the complete wheel is therefore very expensive and time consuming. The aim is to find a method to determine the fatigue properties in more than one position. Such a method is monotonic tensile tests that are both cheap and fast to do and can capture the fatigue properties. Various author[3,4,5,6,7,8,9] have proposed approximate methods whereby a simple monotonic test is used to determine the fatigue properties of a material.

In this project a numerical analysis (Finite Element Analysis or FEA) was performed on a wheel to determine the position of highest stress as well as the value of stress and strain at this position. The numerical analysis was verified by means of experimental analysis in the form of strain gauging. The information obtained from the numerical and experimental analysis was then used to remove a monotonic tensile test sample from the wheel for tensile testing.

The various approximate methods to determine the fatigue life were then implemented by utilising the monotonic tensile test properties.

The various approximate methods were then compared to fatigue tests performed on a full wheel to see which will yield the best first approximation. Four wheel conditions were investigated in this project:

- ❑ Non-heat treated, Unpainted: (abbreviated as UU for future reference)
- ❑ Non-heat treated, Painted: (abbreviated as UP for future reference)
- ❑ Heat treated, Unpainted: (abbreviated as HU for future reference)
- ❑ Heat treated, Painted: (abbreviated as HP for future reference)

The material used was A356 with chemical composition as indicated in Table 1.

For this project the heat treatment consisted of 540°C for 6hrs-solution treatment with quenching in 80°C water for 20s after the solution treatment and ageing at 160°C for 5hrs. The painting process consists of baking the paint on the wheel at 180°C for 15min, 190°C for 25min then finally for 200°C 30min.

Numerical and experimental evaluation.

The FEA was performed on half a wheel that coincides with the plane in which the load is applied in, while the inside rim flange is fixed to simulate the conditions showed in Figure 3. Figure 1 shows a typical FEA Von Mises stress plot with the strain-

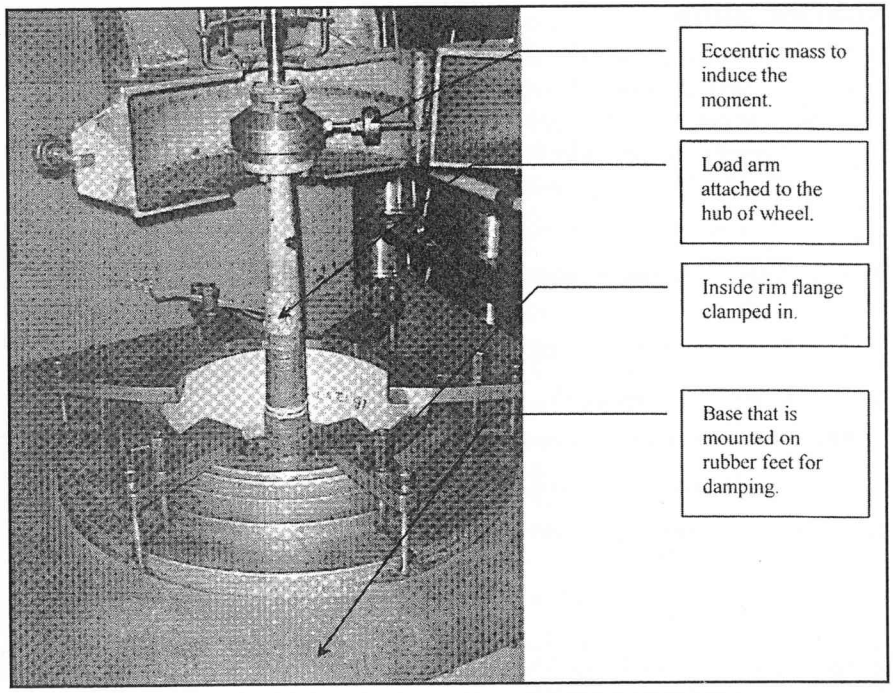

Figure 3. Mechanical wheel fatigue testing machine showing the test set-up

Condition, averaged values	ε_{eng} Elongation [%]	ε_f Fracture ductility [%]	σ_{yield} Yield stress [MPa]	σ_{uts} Tensile Tensile strength [MPa]	σ_f True fracture stress [MPa]	K Strength coefficient [MPa]	n, Strain-hardning exponent
UU	5.336	8.716	109.182	182.092	199.698	319.899	0.191
UP	5.089	9.126	110.292	182.288	200.406	314.531	0.186
HU	3.158	5.052	181.142	224.118	236.340	347.285	0.130
HP	3.119	6.640	200.133	242.330	260.625	345.737	0.103

Table 2. Average monotonic tensile test results for all four conditions[10]

gauged wheel next to it. The strain gauge results were found to be within 8% of the FEA results.[10] The position of the highest stress can now be established, in order to remove the monotonic tensile test sample from the correct position.

Monotonic tensile test set-up and results.

Monotonic tensile samples were removed from the wheel spoke in the same area as was predicted by the numerical analysis. This is shown in Figure 2.

A total of 20 samples were used for every post treatment condition to obtain the tensile properties. The samples were tested on a Hounsfield 100K-C tensile test machine. The average values for each condition are given in Table 2. The elastic modulus was determined by means of strain gauging and applied load on the sample during tensile testing. The average elastic modulus was calculated as 69.03 GPa[10].

Fatigue test setup and results

The fatigue test setup for the complete wheel mounted in position on a wheel fatigue machine is shown in Figure 3.

Before mounting, the wheel's surface was first painted with a mixture of ZnO_2 and glycerin in the region of highest stress, to indicate any crack initiation easily.

A digital camera was also mounted in such a way to capture the fatigue process; this technique ensures repeatability and the ability to do tests without the help of an operator. A total of 46 wheels were tested. On average a test lasted 45 hours.

An example of the digital photos gathered from a typical test is shown in Figure 4. The resolution achieved by this method was 0.3mm.

The first crack (0.3mm–4.62mm with an average of 2.02mm)[10] noticed in this fashion using the digital camera was used to determine the crack initiation life. The wide scatter in crack initiation lengths could be explained if crack initiation and coalescing of pores and/or cracks should occur in between photo shots.

The criterion used for determining the final fracture or point of destruction was an increase in deflection of the load arm of 20%.[11] The test may also be stopped due to internal settings in the fatigue test machine mainly to protect the machine. This was then noted as the point of final fracture.

The results obtained for crack initiation life and total life are shown in Figure 5 and 6. Equivalent stress shown in Figure 5 and 6 is defined in Equation 1.[12]

$$\sigma_{eq} = \sqrt{\sigma_X^2 - \sigma_X \cdot \sigma_Y + \sigma_Y^2 + 3 \cdot \tau_{XY}^2} \qquad (1)$$

Combining the fatigue and monotonic tensile results.

Three approximate methods to relate actual fatigue data to monotonic tensile material test results are compared here. These methods are shown in Equation 2[5],3[7] and 4[8]. Graphically the results of the approximate methods are shown in Figures 7,8,9,10,11 and 12.

- Original universal slopes method by Manson

$$\Delta\varepsilon_T = 3.5 \cdot \frac{\sigma_{uts}}{E} \cdot N_f^{-0.12} + \varepsilon_f^{0.6} \cdot N_f^{-0.6} \qquad (2)$$

- Modified universal slopes method by Muralidharan and Manson

$$\Delta\varepsilon_T = 1.17 \cdot \left(\frac{\sigma_{uts}}{E}\right)^{0.832} \cdot N_f^{-0.09} + 0.0266 \cdot \varepsilon_f^{0.155} \cdot \left(\frac{\sigma_{uts}}{E}\right)^{-0.53} \cdot N_f^{-0.56} \qquad (3)$$

- Uniform material law by Bäumel and Seeger

$$\frac{\Delta\varepsilon_T}{2} = 1.67 \cdot \frac{\sigma_{uts}}{E} \cdot \left(2 \cdot N_f\right)^{-0.095} + 0.35 \cdot \left(2 \cdot N_f\right)^{-0.69} \qquad (4)$$

N_f is numerically solved by substituting ε_{eq} gas defined in Equation 5[12] for $\frac{\Delta\varepsilon_T}{2}$ and using the values in Table 2[10].

Condition of material and fatigue life type.	Manson, standard deviation [log (cycles)]	Muralidharan and Manson, standard deviation [log(cycles)]	Bäumel and Seeger, standard deviation [log (cycles)]
UU, crack initiation	0.306§	1.670	1.107
UP, crack initiation	0.287§	1.315	0.769
UU, total life	0.640§	0.633	0.238
UP, total life	0.731§	0.576	0.249
HU, total life	0.407§	1.041	0.728
HP, total life	0.161§	1.084	0.888
Average	0.422	1.053	0.663

Table 3. Table showing the standard deviations for the approximation methods.[10]

$$\varepsilon_{eq} = \frac{\sqrt{\varepsilon_X^2 - \varepsilon_X \cdot \varepsilon_Y + \varepsilon_Y^2 + \frac{3 \cdot \gamma_{XY}^2}{4}}}{1+\nu} \quad (5)$$

The best first approximation was determined statistically by calculating the standard deviation for each method compared to the fatigue tests. Equation 6 shows the basis for this calculation[10].

$$s = \sqrt{\frac{\sum_{i=1}^{n} \left(\log(N_f) - \log(N_{true})\right)^2}{n-1}} \quad (6)$$

Table 3 lists the values calculated for every material condition and approximate method. The (§) superscript for the calculated standard deviation indicates the most conservative approximation of the fatigue life out of the approximation methods used here.

Discussion of results

The approximate methods can be used as an alternative to full fatigue testing of finished aluminium wheels. This is achieved by removing a test sample from the area where the fatigue properties are needed for monotonic tensile testing. Care is needed when the position and orientation of the tensile sample is determined. This will ensure suitable fatigue/material properties being captured.

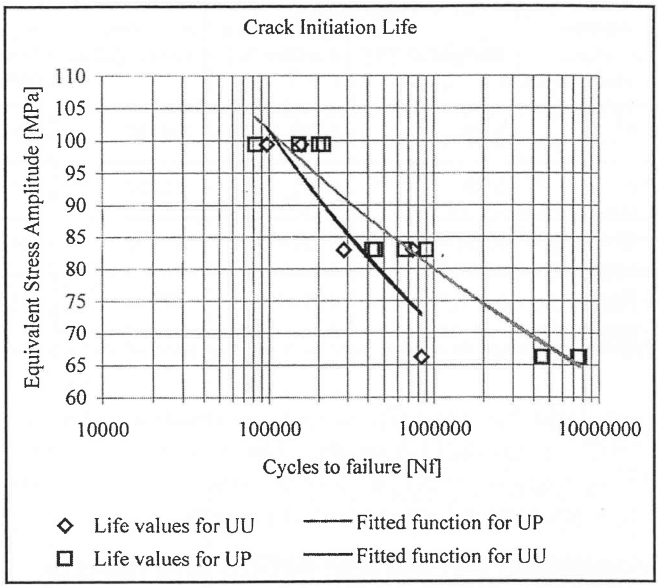

Figure 5. Graph showing the crack initiation life for non-heat treated wheel samples

The universal slopes method by Manson could be used on A356 cast aluminium wheels to obtain a first approximation of the fatigue properties. This method also proved to be the most conservative in the sense that it under estimates the fatigue life.

Comparing the total life with the crack initiation life of wheels as shown in Figure 13, it can also be concluded that the painting of the wheel used in the project or some process associated therewith could increase the crack initiation life of the part.

The painting process is essentially an aging process that will increase the precipitation of fine β'(Mg_2Si) particles, this will improve the strength properties.[13] The chemical or other possible secondary treatment prior to the actual painting of the wheel could also act upon the surface of the wheel to increase its fatigue properties. This should be clear when the monotonic tensile properties of the UU and UP samples are compared with the crack initiation life results that show virtually no improvement on monotonic tensile properties, but some improvement in the crack initiation life results. This effect cannot be simulated accurately on the monotonic tensile sample due to its small size and the risk of over aging.

It is therefore further proposed to do crack initiation fatigue testing on various surface treatment condi-

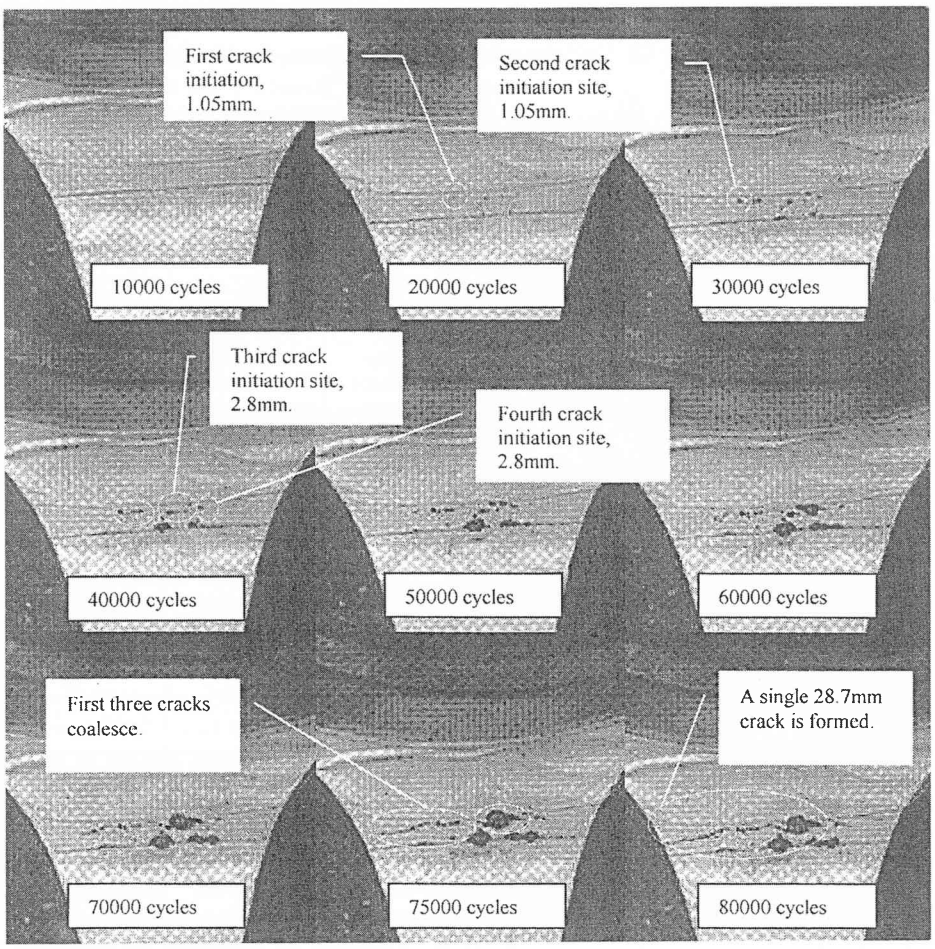

Figure 4. Collage of photos showing the crack initiation and crack propagation in a wheel spoke

tions. The results can be microscopically investigated to distinguish between geometrical, chemical and secondary treatment effects.

References

1 Stanzl-Tschegg, S.E., Mayer, H.R., Beste, A., Kroll, S., "Fatigue and fatigue propagation in AlSi7Mg cast alloys under in-service loading conditions", International Journal of Fatigue, Vol 17, No. 2, pp. 149-155, 1995.

2 Gall, K., Yang, N., Horstmeyer, M., McDowell, D.L., Fan, J., "The influence of modified intermetallics and Si particles on fatigue crack paths in a cast A356 Al alloy", Fatigue Fract Engng Mater Struct 23, pp. 159-172, 1999.

3 Tavernelli, J.F., and Coffin L.F., "Experimental Support for Generalized Equation Predicting Low cycle Fatigue", and Manson, S.S., Discussion, Trans. ASME, J. Basic Eng., vol. 84, no. 4, pp533-537.

4 Heywood, R.B., "Designing against fatigue.", Chapman and Hall, London, 1962

5 Manson, S.S., "Fatigue: A Complex Subject – Some Simple Approximations", Experimental Mechanics, Vol. 5, No. 7, pp. 193, July 1965.

6 Mitchell, M.R., "Fatigue and Microstructure", American Society for Metals, Metals Pack, OH, p. 385, 1979.

7 Muralidharan, U. and Manson, S.S., "A Modified Universal Slopes Equation for the Estimation of Fatigue Charactistics of Metals", Journal of Engineering Materials and Technology, Vol. 110, pp. 55-58, January 1988.

8 Bäumel, A. Jr. and Seeger, T., "Materials Data for Cyclic Loading", Supplement 1, Elsevier Science Publishers, Amsterdam, 1990.

9 Ong, J.H., International Journal of Fatigue, Vol. 15, pp. 213,

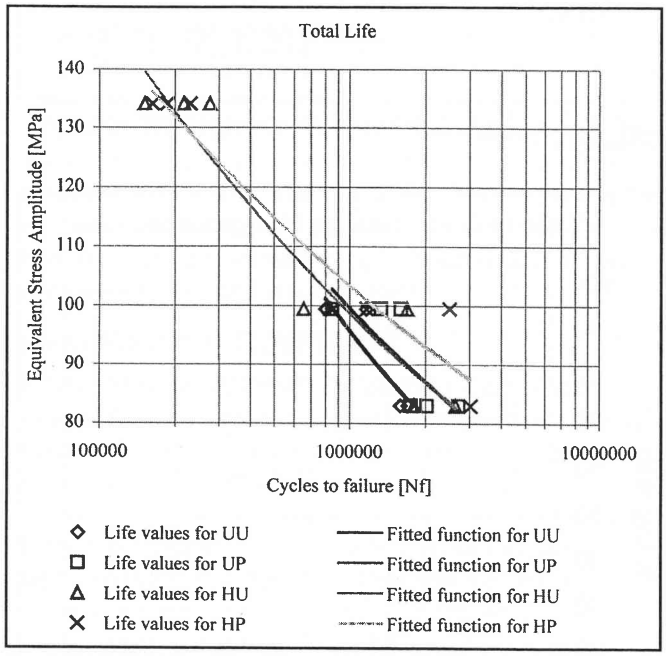

Figure 6. Graph showing the total life for all four conditions

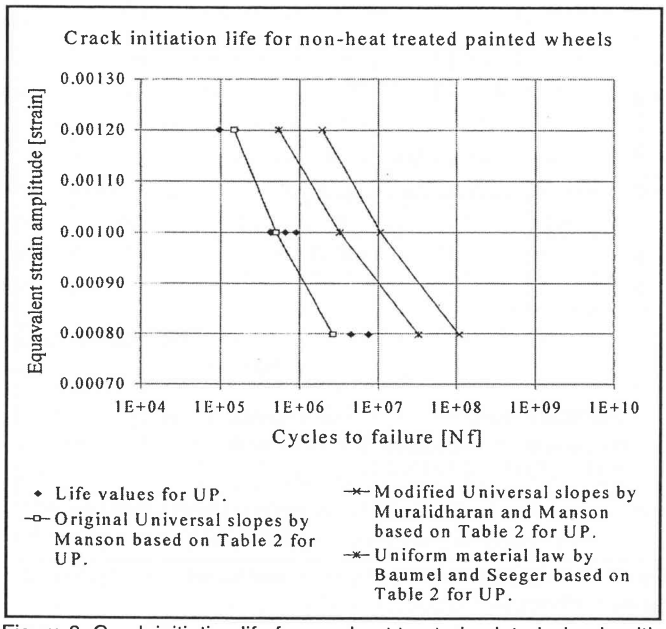

Figure 8. Crack initiation life for non-heat treated painted wheels with approximation methods

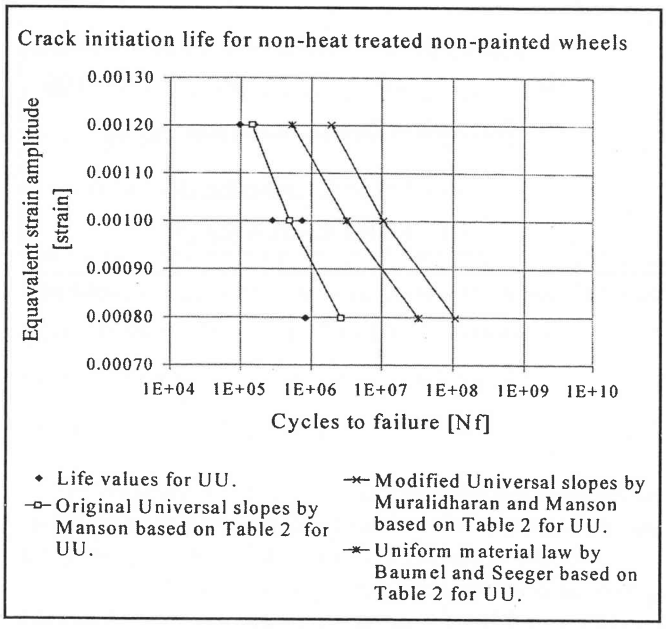

Figure 7. Crack initiation for non-heat treated unpainted wheels with approximation methods

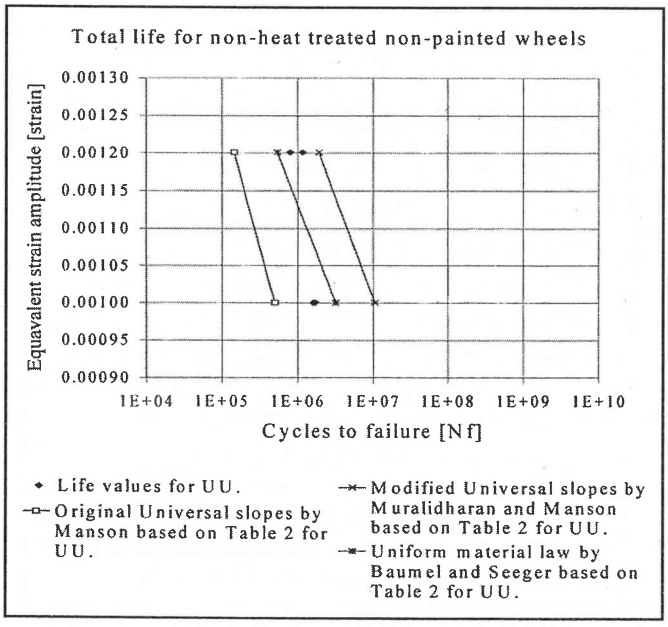

Figure 9. Total life for non-heat treated unpainted wheels with approximation methods

1993.
10 Jacobs, H., "The Fatigue and Tensile Properties of A356 Aluminium Alloy Wheels in Various Post Cast Conditions", Dissertation submitted in partial fulfillment of the requirements for the degree of Magister Ingeneriae in Mechanical Engineering, Rand Afrikaans University, May 2002.
11 Stephens, R.I., Mahoney, B.J., Fossman, R.G, "Low Cycles Fatigue of A356-T6 Cast Aluminium Alloy Wheels", SAE Technical Paper Series, 881707, 1988.
12 Suresh, S., "Fatigue of Materials," 2nd Edition, Cambridge University Press, 1998.
13 Apelian, D., Shivkumar, S., Sigworth, G., "Fundamental Aspects of Heat Treatment of Cast Al-Si-Mg Alloys", AFS Transactions, 727-742, 1989

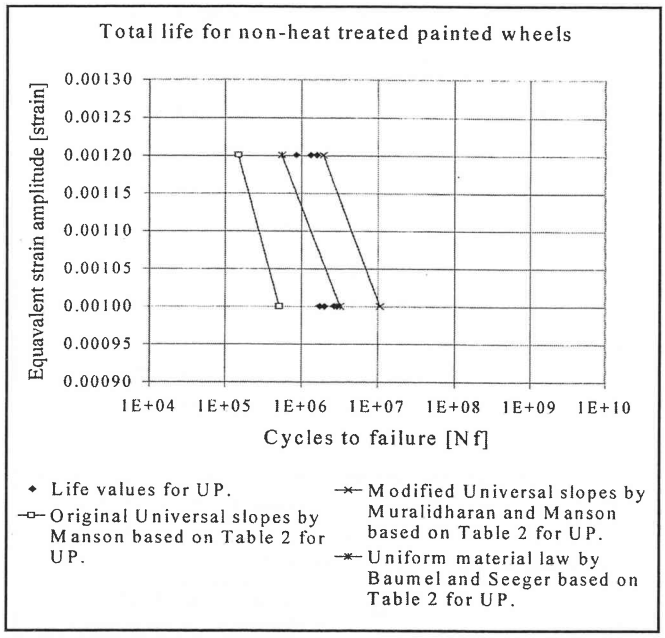

Figure 10. Total life for non-heat treated painted wheels with approximation methods

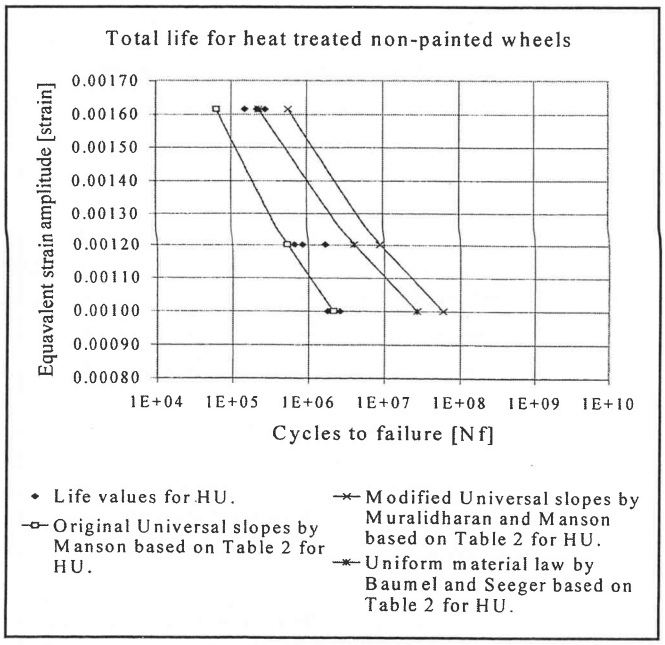

Figure 11. Total life for heat-treated unpainted wheels with approximation methods

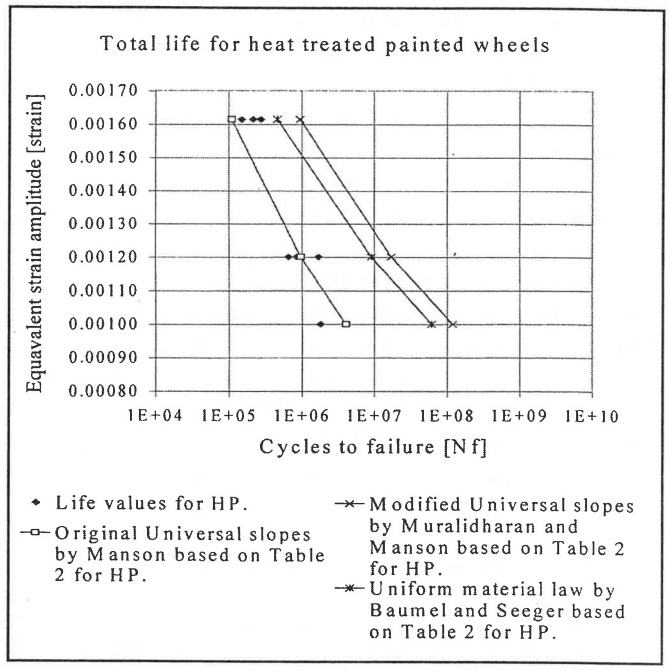

Figure 12. Total life for heat-treated painted wheels with approximation methods

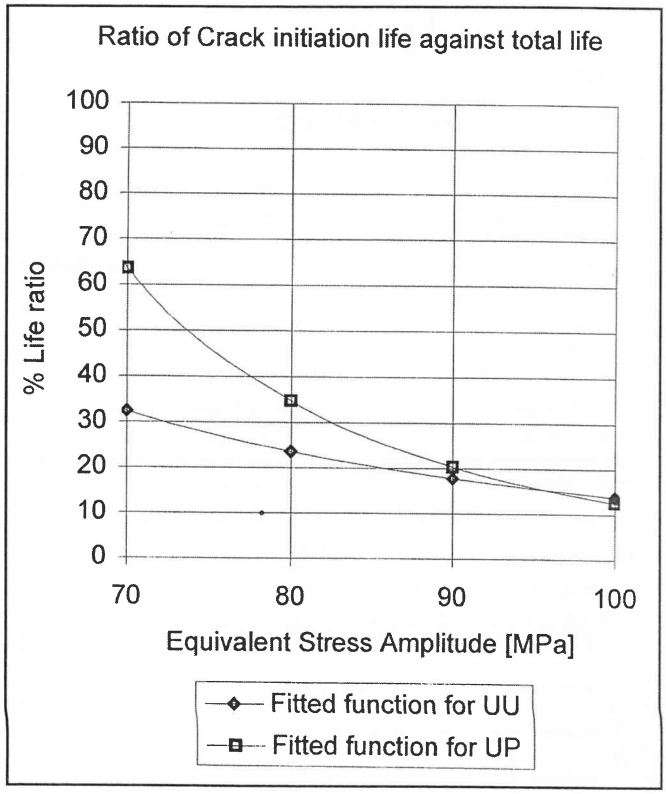

Figure 13. Total life of a wheel as a ratio of the crack initiation life